

On the Design of Digital Blind Feedforward Jitter Free Timing Recovery Schemes for Linear Modulations

Kai Shi, Pradeep K. Sarvepalli and Erchin Serpedin*

Abstract

This paper deals with the compensation of the self-noise (jitter) in a class of nondata aided (blind) feedforward symbol timing recovery schemes for linearly-modulated waveforms transmitted through AWGN channels. The main contribution of this paper is the derivation of a general framework for designing appropriate prefilters to achieve nearly jitter-free digital blind feedforward timing recovery schemes. Computer simulations illustrate that the proposed prefiltering scheme improves significantly the performance of the existing estimators in mid and high SNRs.

Index Terms

timing recovery, feedforward, linear modulation, self-noise, oversampling, prefilter, cyclostationary

Kai Shi, Pradeep K. Sarvepalli and Dr. Erchin Serpedin are with the Dept. of Electrical Engineering, Texas A&M University, College Station, TX 77843-3128, USA. Phone: (979) 458 2287, Fax: (979) 862 3128, email: serpedin@ee.tamu.edu.

*The corresponding author is Dr. Erchin Serpedin. This work was supported by the NSF Award No. CCR-0092901.

I. INTRODUCTION

Symbol timing recovery is a crucial task for digital communication receivers. Nondata-aided (blind) feedforward timing recovery schemes enable fast and reliable synchronization, and therefore, they have found use in burst transmission systems. In [1]-[3], second- or higher-order nonlinearities are utilized in the analog domain to generate spectral lines which contain the symbol timing information. Similar nonlinearities are used in the design of digital blind synchronizers [7]-[8]. We remark also that a general cyclostationary framework that exploits second-order nonlinearities to design digital blind feedforward synchronizers was proposed in [14].

For systems with large excess bandwidth, the performance of the synchronizers that exploit the spectral line generated by a nonlinearity is asymptotically (large sample) very close to the Cramer-Rao bound. If the excess bandwidth is small, significant jitter is induced by data pattern which degrades the performance of the timing recovery scheme in mid and high SNRs [4].

Franks and Bubrouski found that the analog second-order nonlinearity based timing synchronizer can be jitter-free if an appropriate prefilter is used [2]. Reference [6] extended Franks and Bubrouski result to analog synchronizers that assume arbitrary nonlinearities. For digital timing recovery, [11]-[12] exploited similar prefilters to improve the performance of Gardner's nondata aided timing recovery scheme [7]. By means of simulation results, [10] reported that a similar prefilter could be used to improve the performance of the four samples per symbol based feedforward scheme [8]. However, no rigorous theoretical analysis was conducted in [10] to justify the jitter-free timing recovery condition.

In this paper, we derive a closed-form expression for the power of self-noise present in a class of digital blind feedforward timing estimators that rely on the second-order cyclostationary statistics of the received waveform. This rigorous derivation of the self-noise power is later exploited for designing prefilters that ensure nearly jitter-free timing recovery schemes. The proposed analysis and design framework is fairly general and applies not only to feedforward timing recovery schemes that assume oversampling factors larger than or equal to three (see e.g., [8]), but also to clock recovery schemes that assume two samples per symbol [15], [18], which are known to exhibit reduced computational and implementation complexity. In essence, it is shown that if the Franks-Bubrouski condition is fulfilled, i.e., the frequency response of the equivalent pulse is symmetric with respect to half the symbol rate and has bandwidth less than

symbol rate, then a nearly jitter-free digital feedforward timing recovery scheme is obtained for any oversampling factor.

The outline of paper is as follows. The signal model and symbol timing estimators for linearly modulated signals are described in Section II. In Section III, we derive the expression of the self-noise power and design prefilters that provide jitter-free timing recovery schemes. Finally, conclusions are drawn in Section IV, and mathematical derivations are presented in Appendices.

II. SIGNAL MODEL AND SYMBOL TIMING ESTIMATORS

We consider the baseband representation of a linearly modulated signal transmitted through an AWGN channel. The receiver input is expressed as

$$r(t) = \sum_l e^{j2\pi f_e T t} a(l) h_T(t - \epsilon T - lT) + w(t), \quad (1)$$

where $a(l)$ stands for zero-mean unit variance ($E|a(l)|^2 = 1$) independently and identically distributed (i.i.d) complex valued symbols with the fourth-order moment $E[|a(l)|^4] = \gamma$, $h_T(t)$ is the transmitter's filter, and $w(t)$ is complex white Gaussian noise with two-sided power spectral density $N_0/2$. In (1), ϵ and f_e denote the unknown symbol timing delay and frequency offset (normalized by the symbol period T), respectively.

To simplify the analysis, we assume that the frequency offset f_e has been compensated before the timing recovery task is performed (see e.g., [14] for such frequency compensation schemes). Thus, unless otherwise mentioned, f_e is assumed to be zero hereafter. Since the proposed timing delay estimator is insensitive to carrier phase offsets, we also omit the presence of carrier phase offset in (1). After matched filtering with $h_R(T)$, the resulting signal $x_c(t)$ is oversampled by¹ $T_s := T/P$, with the oversampling factor $P \geq 2$, and the received sequence is given by

$$x(n) = \sum_l a(l) h_c(n - lP) + w(n), \quad (2)$$

where $x(n) := x_c(nT_s)$, $w(n) := w(nT_s)$, $h_c(n) := h_c(nT_s)$, $h_c(t) := h_T(t - \epsilon T) \otimes h_R(t)$, and \otimes denotes the convolution operator. We assume that $h_c(t)$ is a raised cosine pulse of bandwidth $[-(1 + \rho)/2T, (1 + \rho)/2T]$, with the roll-off factor ρ ($0 < \rho < 1$) and its Fourier transform (FT) is denoted $H_c(F)$.

¹Notation $:=$ stands for "is defined as".

To estimate the timing offset, the second-order cyclostationary statistics of an observation vector with N symbols will be exploited. The sample cyclic correlation coefficient at cycle k and lag τ is given by

$$\hat{R}_x(k, \tau) = \frac{1}{NP} \sum_{n=0}^{NP-\tau-1} x^*(n)x(n+\tau)e^{-j2\pi kn/P}, \quad (3)$$

where $*$ denotes the conjugation operator. Based on (3), a general estimator² was derived by Gini and Giannakis [14] for oversampling factors $P \geq 3$

$$\hat{\epsilon} = -\frac{1}{2\pi} \arg \left\{ \sum_{\tau=-L_g}^{L_g} G^{-1}(\tau) \hat{R}_x(1, |\tau|) \right\}, \quad (4)$$

where $G(\tau)$ is a real and even function defined by

$$G(\tau) := \frac{P}{T} \int_{-1/2T}^{1/2T} H_c(F - \frac{1}{2T}) H_c(F + \frac{1}{2T}) e^{j2\pi\tau TF/P} dF. \quad (5)$$

The upper limit L_g of summation (4) is fixed as the maximum lag τ that provides a non-trivial value for $|G(\tau)| (\gg 0)$. In (4), L_g cyclic correlations $\hat{R}_x(1, \tau)$ are averaged with weighting factors $G^{-1}(\tau)$. Later we will show that the weighting factors in (4) can be selected to achieve jitter-free timing recovery in the presence even of a finite number of samples (N).

Simulation results in [16] indicate that estimator (4) with small L_g exhibits good performance. In [17], the authors find that the Oerder-Meyer (O&M) estimator [8], a special version ($L_g = 0$) of (4), is asymptotically (for large N) the best estimator among all estimators ($P \geq 3$) using different L_g . Also, the O&M estimator enjoys the property that asymptotically in the number of samples ($N \rightarrow \infty$) is jitter-free [8]. In the finite sample regime ($N < \infty$), we show that an appropriately designed prefilter can ensure almost jitter-free operation of the O&M estimator. Furthermore, we prove that the same prefilter ensures jitter-free operation of the two-samples per symbol based timing recovery schemes [15], [16].

Therefore, we introduce herein the following symbol timing estimators³

$$\hat{\epsilon} = -\frac{1}{2\pi} \arg \{ \Gamma(\epsilon) \}, \quad (6)$$

$$\Gamma(\epsilon) = \begin{cases} \hat{R}_x(1; 0), & P \geq 3 \\ \hat{R}_x(1; 0)G^{-1}(0) - j\Re\{\hat{R}_x(1; 1)\}G^{-1}(1), & P = 2. \end{cases}$$

²This is not the original version but an equivalent version of the estimator proposed in [14].

³Notations $\Re\{\cdot\}$ and $\Im\{\cdot\}$ denote the real and imaginary part, respectively.

The performance of the above estimators is very close to modified Cramer-Rao bound (MCRB) for large roll-off factors ρ . However, for small ρ , a large error floor will be caused by self-noise, a fact which can be observed in Figs. 1 and 3 for oversampling factors $P = 4$ and $P = 2$, respectively. To remove this self-noise, we introduce a prefilter $h_{pre}(t)$ with FT $H_{pre}(F)$. Since this paper focuses on the compensation of self-noise, we omit the additive noise hereafter. Thus, we replace $h_c(n)$ in (2) with $h(n) := h_1(nT_s - \epsilon T)$, where $h_1(t) := h_c(t) \otimes h_{pre}(t)$. Also, in (5), $H_c(F)$ is replaced with $H_1(F) := H_c(F)H_{pre}(F)$, the FT of real-valued filter $h_1(t)$, which is an even function.

III. SELF-NOISE AND NEARLY JITTER-FREE PREFILTER

The bias of estimators (6) can be expressed as

$$\epsilon - \hat{\epsilon} = \frac{1}{2\pi} \arg\{\Gamma(\epsilon)e^{j2\pi\epsilon}\}. \quad (7)$$

Taking the tan-function of both sides of (7), we obtain

$$\tan[2\pi(\epsilon - \hat{\epsilon})] = \frac{\Im\{\Gamma(\epsilon)e^{j2\pi\epsilon}\}}{\Re\{\Gamma(\epsilon)e^{j2\pi\epsilon}\}} \approx 2\pi(\epsilon - \hat{\epsilon}), \quad (8)$$

where the last approximation holds whenever the bias is small since $\tan(x) \approx x$ for $|x| \ll 1$.

Therefore, we can express the square of bias as

$$4\pi^2(\epsilon - \hat{\epsilon})^2 \approx \frac{\Im^2\{\Gamma(\epsilon)e^{j2\pi\epsilon}\}}{\Re^2\{\Gamma(\epsilon)e^{j2\pi\epsilon}\}} = \frac{Q_{ss}}{I_{ss}}, \quad (9)$$

where $I_{ss} := \Re^2\{\Gamma(\epsilon)e^{j2\pi\epsilon}\}$ and $Q_{ss} := \Im^2\{\Gamma(\epsilon)e^{j2\pi\epsilon}\}$ represent the in-phase and quadrature components of the self-noise, respectively.

A. Case I: Oversampling Factors $P \geq 3$

In the Appendix-A, the expectation of quadrature part of self-noise is expressed as

$$E[Q_{ss}] = \frac{P^2}{4T^3} \int_{-1/2T}^{1/2T} [(\gamma - 2)Q_1(V) + Q_2(V)] \frac{\sin^2(\pi NVT)}{\pi^2 V^2} dV, \quad (10)$$

where:

$$\begin{aligned} Q_1(V) &:= \int_{-1/2T}^{1/2T} \int_{-1/2T}^{1/2T} U_Q(F_1, V) U_Q(-F_2, V) dF_1 dF_2, \\ Q_2(V) &:= \frac{1}{T} \int_{-1/2T}^{1/2T} U_Q^2(F, V) dF, \\ U_Q(F, V) &:= H_2(F, V) - H_2(-F, -V), \\ H_2(F, V) &:= H_1\left(F - \frac{1}{2T} - V\right) H_1\left(F + \frac{1}{2T}\right). \end{aligned} \quad (11)$$

Similarly, the in-phase part of self-noise can be expressed as

$$E[I_{ss}] = N^2[G(0)]^2 + \frac{P^2}{4T^3} \int_{-1/2T}^{1/2T} [(\gamma - 2)I_1(V) + I_2(V)] \frac{\sin^2(\pi NVT)}{\pi^2 V^2} dV, \quad (12)$$

where:

$$\begin{aligned} I_1(V) &:= \int_{-1/2T}^{1/2T} \int_{-1/2T}^{1/2T} U_I(F_1, V) U_I(-F_2, V) dF_1 dF_2, \\ I_2(V) &:= \frac{1}{T} \int_{-1/2T}^{1/2T} U_I^2(F, V) dF, \\ U_I(F, V) &:= H_2(F, V) + H_2(-F, -V). \end{aligned}$$

Since $E[I_{ss}]$ is much larger than $E[Q_{ss}]$ and the first term of $E[I_{ss}]$ is dominant, we can make the following approximation:

$$E[4\pi^2(\epsilon - \hat{\epsilon})^2] \approx \frac{E[Q_{ss}]}{E[I_{ss}]} \approx \frac{E[Q_{ss}]}{N^2[G(0)]^2}. \quad (13)$$

If we interpret the rectangular discrete Fourier transform (DFT) processing window as an equivalent analog bandpass filter with frequency support centered around $1/T$, (11)-(12) are close in form to the results regarding the self-noise in analog synchronizers (delay $\Delta = 0$) [5]. Based on the previous results, the following remarks can be drawn. Observing that $G(0)$ is proportional to P , we find that the self-noise power is independent of the over-sampling factor P for $P \geq 3$. If the length of the observation vector is infinite ($N \rightarrow \infty$), the FT of rectangular window (sinc-function present in (10)) becomes $\delta(V)$. Since $H_1(F)$ is an even function, $U_Q(F, 0) = 0$, which leads to $Q_1(0) = Q_2(0) = 0$, and thus, $E[Q_{ss}] = 0$. In other words, we re-obtain the conclusion stated in [8], namely that this estimator is asymptotically jitter-free. A more important conclusion is that if we choose a proper prefilter $H_{pre}(F)$ such that $H_1(F)$ is symmetric around $1/2T$ and with bandwidth less than $1/T$, then $U_Q(F, V)$ and $E[Q_{ss}]$ are found to be zero. Thus, the resulting estimator is nearly⁴ jitter-free even for finite (small) N . Since large excess bandwidth is helpful for estimator's performance with respect to (w.r.t) additive noise [5] and [16], we make use of the same prefilter as [11]

$$h_{pre}(t) = h_c(t) \cos(2\pi t/T), \quad (14)$$

such that the largest excess bandwidth is preserved.

⁴It is not purely jitter-free because of the approximations made in (8) and (13).

In Fig. 1, we compare the performance of estimators with and without prefilter for systems with low roll-off factors ($\rho = 0.25$) using Monte-Carlo simulations. Henceforth, all simulation results are obtained by performing 1,000 Monte-Carlo runs for each SNR value assuming 100 symbols for each trial. At mid and high SNRs where the performance is dominated by the self-noise, no error floor is observed for the estimator with prefilter and its performance is closer to the MCRB [13]. At low SNRs where the additive noise is dominant, the prefilter does not degrade the performance since the same excess bandwidth is preserved.

If $h_{pre}(t)$ is replaced by an equivalent FIR $h_{pre}(n)$ with $L_P + 1$ taps, the estimator (6) can be expressed as

$$\hat{\epsilon} = -\frac{1}{2\pi} \arg \left[\sum_{\tau=-L_P}^{L_P} r_{h_{pre}}(\tau) \hat{R}_x(1, |\tau|) \right], \quad (15)$$

where $r_{h_{pre}}(\tau) := \sum_{\tau_1=|\tau|}^{L_P+|\tau|} h_{pre}(\tau_1) h_{pre}^*(\tau_1 - |\tau|)$ can be viewed as the autocorrelation coefficient at lag τ of the impulse response of the prefilter. Thus, to remove the self-noise, the $2L_P + 1$ cyclic correlations in (4) should be averaged with weighting factors that depend on the prefilter's autocorrelation coefficients.

B. Case II: The Oversampling Factor $P = 2$

The expectation of Q_{ss} and I_{ss} for $P = 2$ are calculated in Appendix-B. Since the first term of $E[I_{ss}]$ is much larger than other terms present in $E[I_{ss}]$ and $E[Q_{ss}]$, we can also make the following approximation

$$E[4\pi^2(\epsilon - \hat{\epsilon})^2] \approx \frac{E[Q_{ss}]}{E[I_{ss}]} \approx \frac{E[Q_{ss}]}{N^2[G(1)G(0)]^2}. \quad (16)$$

If the same prefilter as in the previous case ($P \geq 3$) is used, after some lengthy algebra, it is found

$$E[Q_{ss}] = \sin^2(4\pi\epsilon) \int_{-1/2T}^{1/2T} \left[\frac{4}{T^4} Q_2(V) + (\gamma - 2) \frac{8}{T^3} Q_3(V) \right] \frac{\sin^2(\pi NVT)}{\pi^2 V^2} dV, \quad (17)$$

where

$$Q_2(V) = \int_{-1/2T}^{1/2T} [G^2(0) + G^2(1) - 2G(0)G(1)\cos(\pi FT)] H_2^2(F, V) dF, \quad (18)$$

$$Q_3(V) = \int_{-1/2T}^{1/2T} \int_{-1/2T}^{1/2T} H_2(F_1, V) H_2(F_2, -V) [G^2(0) + G^2(1) - 2G(0)G(1)\cos(\pi F_1 T)] dF_1 dF_2. \quad (19)$$

Next, we justify that $E[Q_{ss}] \approx 0$. To check $Q_2(V) \approx 0$ and $Q_3(V) \approx 0$, we evaluate numerically the terms involved in (18). In Fig. 2, we plot the ratios $G_m(1,0)/G_m(0,0)$, $m = 1, 2$, for different roll-off factors ρ , where

$$G_m(0, V) := \int_{-1/2T}^{1/2T} H_2^m(F, V) dF,$$

$$G_m(1, V) := \int_{-1/2T}^{1/2T} H_2^m(F, V) \cos(\pi FT) dF.$$

Fig. 2 shows that $G_m(1,0)/G_m(0,0)$ is very close to 1. Recalling that $G_1(1,0) = G(1)$ and $G_1(0,0) = G(0)$, we can approximate $G(1) \approx G(0)$. Also, we can also approximate $G_m(1, V)/G_m(0, V) \approx 1$ if V is small. Note also that for large V , $\frac{\sin^2(\pi NV T)}{\pi^2 V^2} \approx 0$ in (17), so we can approximate $G_m(0, V) \approx G_m(1, V)$, $m = 1, 2$. By considering all these approximations in (18), it follows that $Q_2(V) \approx 0$ and $Q_3(V) \approx 0$. Thus, $E[Q_{ss}] \approx 0$, which means that the same prefilter can be used for any oversampling factor (including $P = 2$) to remove the self-noise. Simulation results in Fig. 3 assume an oversampling factor $P = 2$ and corroborate the benefits of this prefilter relative to the scheme without prefilter.

Interestingly enough, for the special case $\epsilon = 0$, to obtain jitter-free estimation, the condition $h(n)h(n+1) = 0$ must be satisfied, and this constraint can be used to derive directly the prefilter. A similar result is reported in [11] for Gardner's scheme [7].

IV. CONCLUSIONS

We have derived a closed-form expression for the power of self-noise for a class of blind feedforward symbol timing estimators that assume oversampling factors equal to or larger than 2. It has been shown that an appropriate prefilter after the receiver's matched filter can be utilized to remove the jitter. Simulation results prove that the synchronizer which assumes such a prefilter is nearly jitter-free even in the presence of a finite (reduced) number of samples as long as linear-modulated signals are assumed. Our preliminary simulation results indicate that such prefilters can improve performance of square-law estimators for MSK and GMSK-type signals, a topic which will be researched in a future paper.

Appendix A: Evaluation of Self-Noise Power for $P \geq 3$

We assume without any loss of generality that the transmit symbol stream belongs to an M-QAM or M-PSK modulation with $M > 2$ (the case of a real-valued (BPSK/PAM) modulations

supports only a minor modification). For $P \geq 3$, the quadrature and in-phase components of the jitter can be expressed as:

$$\begin{aligned} Q_{ss} &= \left(\sum_{n=0}^{PN-1} |x(n)|^2 \sin[2\pi(\epsilon - n/P)] \right)^2, \\ I_{ss} &= \left(\sum_{n=0}^{PN-1} |x(n)|^2 \cos[2\pi(\epsilon - n/P)] \right)^2. \end{aligned} \quad (20)$$

Based on the following fact

$$E[a(l_1)a^*(l_2)a(l_3)a^*(l_4)] = \begin{cases} 1, & l_1 = l_2 \neq l_3 = l_4 \\ 1, & l_1 = l_4 \neq l_2 = l_3 \\ \gamma, & l_1 = l_2 = l_3 = l_4 \\ 0, & \text{otherwise} \end{cases} \quad (21)$$

it follows that

$$\begin{aligned} E[|x(m)|^2|x(n)|^2] &= \sum_{l_1} \sum_{l_2} \sum_{l_3} \sum_{l_4} E[a(l_1)a^*(l_2)a(l_3)a^*(l_4)]h(m - l_1P) \\ &\quad \cdot h^*(m - l_2P)h(n - l_3P)h^*(n - l_4P) \\ &= \sum_l \sum_i g_0(m - lP)g_0(n - iP) \quad (= E_1) \\ &\quad + \sum_l \sum_i g_l(m - iP)g_l(n - iP) \quad (= E_2) \\ &\quad + (\gamma - 2) \sum_i g_0(m - iP)g_0(n - iP) \quad (= E_3) \end{aligned} \quad (22)$$

where $g_l(n) := h(n - lP)h^*(n)$. Thus, for $P \geq 3$, we have

$$\begin{aligned} E[I_{ss}] &= \sum_{n=0}^{PN-1} \sum_{m=0}^{PN-1} (E_1 + E_2 + E_3) \cos[2\pi(\epsilon - m/P)] \cos[2\pi(\epsilon - n/P)], \\ E[Q_{ss}] &= \sum_{n=0}^{PN-1} \sum_{m=0}^{PN-1} (E_1 + E_2 + E_3) \sin[2\pi(\epsilon - m/P)] \sin[2\pi(\epsilon - n/P)]. \end{aligned} \quad (23)$$

Following the steps in [16], the first part of $E[Q_{ss}]$ is found

$$\begin{aligned} E_{Q1} &= \sum_{n=0}^{PN-1} \sum_{m=0}^{PN-1} E_1 \sin[2\pi(\epsilon - m/P)] \sin[2\pi(\epsilon - n/P)] \\ &= \{N \sum_l |h(l)|^2 \sin[2\pi(\epsilon - l/P)]\}^2 = 0. \end{aligned} \quad (24)$$

Making use of Parseval's theorem, we find

$$\begin{aligned}
E_{Q2} &= \sum_{n=0}^{PN-1} \sum_{m=0}^{PN-1} E_2 \sin[2\pi(\epsilon - m/P)] \sin[2\pi(\epsilon - n/P)] \\
&= \sum_l \sum_i \left[\sum_m \text{Rect}(NP) g_l(m - iP) \Im[e^{j2\pi(\epsilon - m/P)}] \right]^2 \\
&= -\frac{1}{4} \sum_l \sum_i \left[\int_{-1/2}^{1/2} [H(f + \frac{1}{P})e^{j2\pi\epsilon} - H(f - \frac{1}{P})e^{-j2\pi\epsilon}] H'(f) e^{-j2\pi l f P} df \right]^2, \quad (25)
\end{aligned}$$

where $\text{Rect}(NP)$ is a rectangular window of length NP , $H(f)$ is the FT of $h(n)$ and $H'(f)$ is the convolution of $H(f)$ and the FT of $\text{Rect}(NP)$. For $|f| < 1/2$, it is known that (see e.g., [14], [16])

$$\begin{aligned}
H(f) &= \frac{P}{T} H_1\left(\frac{fP}{T}\right) e^{-j2\pi f P \epsilon}, \quad P \geq 2 \\
H\left(f + \frac{k}{P}\right) &= \frac{P}{T} H_1\left(\frac{fP + k}{T}\right) e^{-j2\pi(fP + k)\epsilon}, \quad P \geq 3
\end{aligned} \quad (26)$$

where $k = \pm 1$. In addition,

$$E_{Q2} = -\frac{1}{4} \sum_l \sum_i \left[\frac{P}{T} \int_{-1/2T}^{1/2T} S_Q(F) e^{-j2\pi l (FT + 1/2)} dF \right]^2,$$

where $S_Q(F)$ is band-limited to $(-\frac{1}{2T}, \frac{1}{2T})$ and given by

$$S_Q(F) := H'_1\left(F - \frac{1}{2T}\right) H_1\left(F + \frac{1}{2T}\right) - H'_1\left(F + \frac{1}{2T}\right) H_1\left(F - \frac{1}{2T}\right), \quad (27)$$

$$H'_1(F) := \int_{-1/2T}^{1/2T} H_c(F - V) \frac{\sin(\pi NVT)}{\pi V} e^{j2\pi(i - N/2 + \epsilon)VT} dV. \quad (28)$$

Making use of Poisson's formula:

$$\sum_l e^{-j2\pi l (F_1 + F_2)T} = \frac{1}{T} \sum_k \delta\left(F_1 + F_2 - \frac{k}{T}\right),$$

and the fact that $S_Q(F)$ is band-limited, it follows that

$$\begin{aligned}
E_{Q2} &= -\frac{1}{4} \frac{P^2}{T^2} \int_{-1/2T}^{1/2T} \int_{-1/2T}^{1/2T} \sum_i S_Q(F_1) S_Q(F_2) \sum_l e^{-j2\pi l (F_1 + F_2)T} dF_1 dF_2 \\
&= -\frac{P^2}{4T^3} \int_{-1/2T}^{1/2T} \sum_i S_Q(F) S_Q(-F) dF, \quad (29)
\end{aligned}$$

and

$$\begin{aligned}
\sum_i S_Q(F_1)S_Q(F_2) &= \int_{-1/2T}^{1/2T} \int_{-1/2T}^{1/2T} U_Q(F_1, V_1)U_Q(F_2, V_2)e^{j2\pi(\epsilon - \frac{N}{2})(V_1+V_2)T} \\
&\quad \cdot \frac{\sin(\pi NV_1 T)}{\pi V_1} \frac{\sin(\pi NV_2 T)}{\pi V_2} \sum_i e^{j2\pi i(V_1+V_2)T} dV_1 dV_2 \\
&= \frac{1}{T} \int_{-1/2T}^{1/2T} U_Q(F_1, V)U_Q(F_2, -V) \frac{\sin^2(\pi NV T)}{\pi^2 V^2} dV.
\end{aligned} \tag{30}$$

Using $U_Q(F, -V) = -U_Q(-F, V)$, it follows that

$$E_{Q2} = \frac{P^2}{4T^4} \int_{-1/2T}^{1/2T} \int_{-1/2T}^{1/2T} U_Q^2(F, V) dF \frac{\sin^2(\pi NV T)}{\pi^2 V^2} dV.$$

Similarly, the third part of $E[Q_{ss}]$ is expressed as

$$\begin{aligned}
E_{Q3} &= \sum_{n=0}^{PN-1} \sum_{m=0}^{PN-1} E_3 \sin[2\pi(\epsilon - m/P)] \sin[2\pi(\epsilon - n/P)] \\
&= \frac{(\gamma - 2)P^2}{4T^3} \int_{-1/2T}^{1/2T} T_Q(V) \frac{\sin^2(\pi NV T)}{\pi^2 V^2} dV.
\end{aligned}$$

Appendix B: Self-noise Power for $P = 2$

When $P = 2$, it follows

$$\begin{aligned}
Q_{ss} &= G^2(0)\cos^2(2\pi\epsilon)A + G^2(1)\sin^2(2\pi\epsilon)B - G(0)G(1)\sin(4\pi\epsilon)C, \\
I_{ss} &= G^2(0)\sin^2(2\pi\epsilon)A + G^2(1)\cos^2(2\pi\epsilon)B + G(0)G(1)\sin(4\pi\epsilon)C,
\end{aligned} \tag{31}$$

where

$$\begin{aligned}
A &:= \sum_{n=0}^{PN-2} \sum_{m=0}^{PN-2} \Re[x^*(n)x(n+1)]\Re[x^*(m)x(m+1)]e^{\frac{-j2\pi(n+m)}{P}}, \\
B &:= \sum_{n=0}^{PN-1} \sum_{m=0}^{PN-1} |x(n)|^2|x(m)|^2e^{\frac{-j2\pi(n+m)}{P}}, \\
C &:= \sum_{n=0}^{PN-2} \sum_{m=0}^{PN-1} \Re[x^*(n)x(n+1)]|x(m)|^2e^{\frac{-j2\pi(n+m)}{P}}.
\end{aligned} \tag{32}$$

In [16], when $P = 2$ and $k = \pm 1$, it is found that

$$H(f + \frac{k}{2}) = \frac{2}{T} [H_1(\frac{2f+k}{T})e^{-j2\pi\epsilon} + H_1(\frac{2f-k}{T})e^{j2\pi\epsilon}]e^{-j4\pi kf\epsilon}. \tag{33}$$

Following the steps in Appendix-A, it follows that

$$E[A] = E[A_1] + E[A_2] + E[A_3], \tag{34}$$

and

$$\begin{aligned}
E[A_1] &= G^2(1)\sin^2(2\pi\epsilon)N^2, \\
E[A_2] &= -\frac{4}{T^4} \int_{-1/2T}^{1/2T} \int_{-1/2T}^{1/2T} U_A(F, V)U_A(-F, -V)dF \frac{\sin^2(\pi NVT)}{\pi^2 V^2} dV, \\
E[A_3] &= \frac{-4(\gamma - 2)}{T^3} \int_{-1/2T}^{1/2T} U_{A3}(V) \frac{\sin^2(\pi NVT)}{\pi^2 V^2} dV,
\end{aligned}$$

where

$$\begin{aligned}
U_A(F, V) &:= H_2(F, V)e^{-j2\pi\epsilon} - H_2(-F, -V)e^{j2\pi\epsilon}, \\
U_{A3}(V) &:= \int_{-1/2T}^{1/2T} \int_{-1/2T}^{1/2T} U_A(F_1; V)U_A(F_2; -V)dF_1 dF_2.
\end{aligned}$$

The expectation of B can be expressed as

$$E[B] = E[B_1] + E[B_2] + E[B_3], \quad (35)$$

and

$$\begin{aligned}
E[B_1] &= G^2(0)\cos^2(2\pi\epsilon)N^2, \\
E[B_2] &= \frac{4}{T^4} \int_{-1/2T}^{1/2T} \int_{-1/2T}^{1/2T} U_B(F, V)U_B(-F, -V)dF \frac{\sin^2(\pi NVT)}{\pi^2 V^2} dV, \\
E[B_3] &= \frac{4(\gamma - 2)}{T^3} \int_{-1/2T}^{1/2T} U_{B3}(V) \frac{\sin^2(\pi NVT)}{\pi^2 V^2} dV,
\end{aligned}$$

where

$$\begin{aligned}
U_B(F, V) &:= H_2(F, V)e^{-j2\pi\epsilon} + H_2(-F, -V)e^{j2\pi\epsilon}, \\
U_{B3}(V) &:= \int_{-1/2T}^{1/2T} \int_{-1/2T}^{1/2T} U_B(F_1; V)U_B(F_2; -V)dF_1 dF_2.
\end{aligned}$$

The expectation of C is computed as

$$E[C] = E[C_1] + E[C_2] + E[C_3], \quad (36)$$

and

$$\begin{aligned}
E[C_1] &= (1/2)G(0)G(1)\sin(4\pi\epsilon)N^2, \\
E[C_2] &= \frac{4j}{T^4} \int_{-1/2T}^{1/2T} \int_{-1/2T}^{1/2T} U_C(F, V)U_C(-F, -V)e^{-j\pi FT} dF \frac{\sin^2(\pi NVT)}{\pi^2 V^2} dV, \\
E[C_3] &= \frac{4j(\gamma - 2)}{T^3} \int_{-1/2T}^{1/2T} U_{C3}(V) \frac{\sin^2(\pi NVT)}{\pi^2 V^2} dV,
\end{aligned}$$

where

$$U_{C3}(V) := \int_{-1/2T}^{1/2T} \int_{-1/2T}^{1/2T} U_A(F_1; V) U_B(F_2; -V) e^{-j\pi F_1 T} dF_1 dF_2. \quad (37)$$

Thus,

$$\begin{aligned} E[Q_{ss}] &= G^2(0)\cos^2(2\pi\epsilon)E[A_2 + A_3] + G^2(1)\sin^2(2\pi\epsilon) \\ &\quad \cdot E[B_2 + B_3] - G(0)G(1)\sin(4\pi\epsilon)E[C_2 + C_3], \\ E[I_{ss}] &= N^2[G(1)G(0)]^2 + G^2(0)\sin^2(2\pi\epsilon)E[A_2 + A_3] \\ &\quad + G^2(1)\cos^2(2\pi\epsilon)E[B_2 + B_3] + G(0)G(1)\sin(4\pi\epsilon)E[C_2 + C_3]. \end{aligned} \quad (38)$$

REFERENCES

- [1] W. R. Bennet, "Statistics of regenerative digital transmission," *Bell Syst. Tech. J.*, vol. 37, pp. 1501-1542, Nov. 1958.
- [2] L. E. Franks and J. P. Bubroski, "Statistical properties of timing jitter in a PAM timing recovery scheme," *IEEE Trans on Comm.*, vol. COM-22, pp. 913-920, July 1974.
- [3] J. E. Mazo, "Jitter comparison of tones generated by squaring and by fourth-power circuits," *Bell Syst. Tech. J.*, vol. 57, pp. 1489-99, May-June 1978.
- [4] F. M. Gardner, "Self-noise in synchronizers," *IEEE Trans. on Comm.*, vol. COM-28, pp. 1159-63, Aug. 1980.
- [5] A. N. D'Andrea and U. Mengali, "Performance analysis of the delay-line clock regenerator," *IEEE Trans. on Comm.*, vol. COM-34, pp. 321-328, April 1986.
- [6] A. N. D'Andrea, U. Mengali and M. Moro, "Nearly Optimum Prefiltering in Clock Recovery," *IEEE Trans. on Comm.*, vol. COM-34, pp. 1081-88, Nov. 1986.
- [7] F. M. Gardner, "A BPSK/QPSK timing-error detector for samples receivers," *IEEE Trans. on Comm.*, vol. COM-34, pp.423-9, Aug. 1986.
- [8] M. Oerder and H. Meyr, "Digital filter and square timing recovery," *IEEE Trans. on Comm.*, vol.36, pp. 605-612, May 1988.
- [9] T. T. Fang, "I and Q decomposition of self-noise in square-law clock regenerators," *IEEE Trans. on Comm.*, vol. 36, pp. 1044-1052, Sept. 1988.
- [10] K. Schmidt and A. Wittneben, "Systematic complexity reduction for digital square timing recovery," *Proc. 42'VTC*, vol. 1, pp. 283-288, May 1992.
- [11] A. N. D'Andrea, and M. Luise, "Design and analysis of a jitter-free clock recovery scheme for QAM systems," *IEEE Trans. on Comm.*, vol. 41, pp. 1296-1299, Sept. 1993.
- [12] A. N. D'Andrea, and M. Luise, "Optimization of symbol timing recovery of QAM data demodulators," *IEEE Trans. on Comm.*, vol. 44, pp. 399-406, Sept. 1996.
- [13] U. Mengali and A. N. D'Andrea, "Synchronization techniques for digital receivers," *Plenum Press, New York*, 1997.
- [14] F. Gini and G. B. Giannakis, "Frequency offset and symbol timing recovery in flat-fading channels: a cyclostationary approach," *IEEE Trans. Comm.*, vol. 46, pp.400-411, Mar. 1998.
- [15] S. J. Lee, "A new non-data-aided feedforward symbol timing estimator using two samples per symbol," *IEEE Comm. Lett.*, vol. 6, pp. 205-207, May 2002.

- [16] Y. Wang, P. Ciblat, E. Serpedin and P. Loubaton, "Performance analysis of a class of nondata-aided frequency offset and symbol timing estimators for flat-fading channels," *IEEE Trans. on Signal Processing*, vol. 5, pp. 2295-2305, Sept. 2002.
- [17] Y. Wang, E. Serpedin and P. Ciblat, "Blind feedforward cyclostationarity-based timing estimation for linear modulations," *submitted to IEEE Trans. on Wireless Comm.*, 2002.
- [18] Y. Wang, E. Serpedin and P. Ciblat, "An alternative blind feedforward symbol timing estimator using two samplers per symbol," *submitted to IEEE Trans. on Comm.*, 2002.
- [19] Y. Wu and T. Ng, "Symbol timing recovery for GMSK modulation based on square algorithm," *IEEE Comm. Lett.*, vol. 5, pp. 221-223, May 2001.

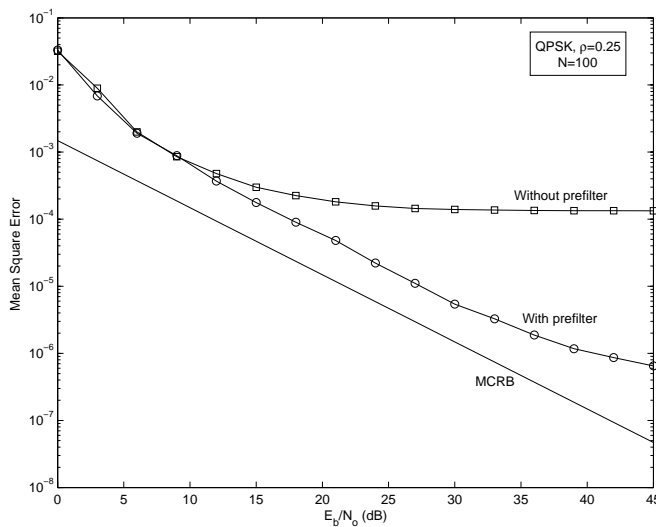


Fig. 1. Comparison of symbol timing estimators for P=4.

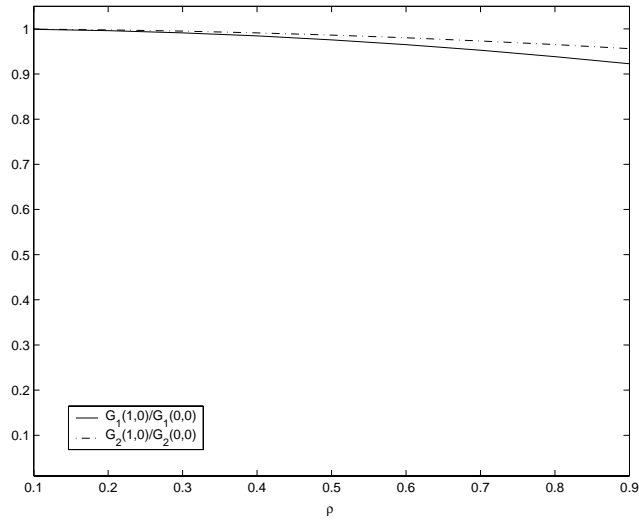


Fig. 2. Plots of $G_m(1,0)/G_m(0,0)$ for $m = 1, 2$ versus various roll-off factors ρ .

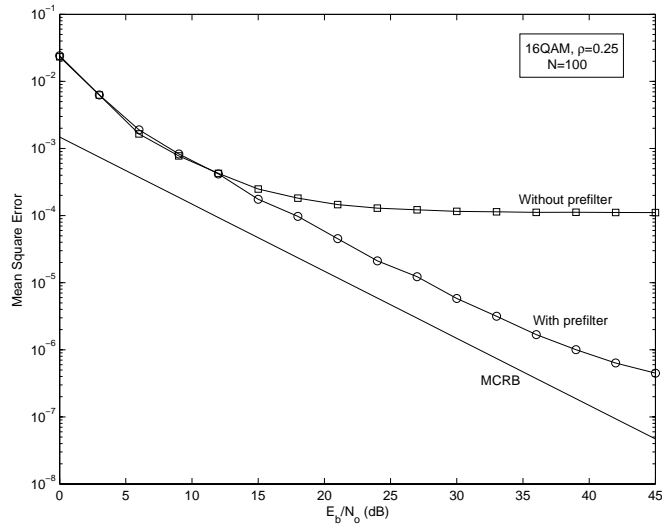


Fig. 3. Comparison of symbol timing estimators for $P = 2$.